International Journal of Current Science, Engineering & Technology ISSN : 2581-4311
Original Research Article | Open Access | AMCT 2017 Malaysia | *Special Issue*

Dielectric Resonator Antenna of Nd-doped $BaTiO_3$ for X-Band Applications

Nik Akmar REJAB[1,a*], Mohamadariff OTHMAN[2,b], Mohd Fariz AB RAHMAN[1,c], Zainal Arifin AHMAD[1,d], Mohd Fadzil AIN[3,e]

[1]Structural Materials Niche Area, School of Materials and Mineral Resource Engineering, Engineering Campus, Universiti Sains Malaysia, 14300, Nibong Tebal, Seberang Perai Selatan, Malaysia.

[2]Department of Electrical Engineering, Faculty of Engineering, University of Malaya, 50603 Kuala Lumpur, Malaysia.

[3]School of Electric and Electronic Engineering, Engineering Campus, Universiti Sains Malaysia, 14300, Nibong Tebal, Seberang Perai Selatan, Malaysia.

[*a]akmarnik@usm.my, [b]mohamadariff@um.edu.my, [c]mohdfarizabrahman@yahoo.com, [d]srzainal@usm.my, [e]eemfadzil@usm.my

ABSTRACT. In this paper, dielectric resonator antenna (DRA) fabricated using neodymium (Nd) doped on barium titanate powder ($Ba_{(1-x)}Nd_xTiO_3$) with x values varying from 0, 0.01, 0.03, 0.05, 0.07 and 0.10 via sol-gel process was investigated. $Ba_{(1-x)}Nd_xTiO_3$ in cylindrical shape with high dielectric constant and low loss tangent was used. A simple microstrip line was utilized as a feeder to ease the fabrication process. A comparative study of the various dope values of Nd with the same dimensions in terms of resonant frequency, return loss, bandwidth as well as radiation pattern were analyzed. Operational frequency of DRA was found to be tunable using different values of doped Nd, but the radiation patterns of the DRA were not very different. This antenna is suitable for use in X-band applications.

***Keyword**: Dielectric resonator antenna, Barium titanate, Neodymium, X-band;*

Received: 15.10.2017, Revised: 15.12.2017, Accepted: 30.02.2018, and Online: 20.03.2018;

DOI: *10.30967/ijcrset.1.S1.2018.596-602*

Selection and/or Peer-review under responsibility of Advanced Materials Characterization Techniques (AMCT 2017), Malaysia.

1. INTRODUCTION

The field of microwave communication has gone through exceptional growth for the last two decades. This is driven by the latest trend of technology miniaturization which demands the enhancement of technology versatility to accommodate various technological constraints. The dielectric resonator antenna (DRA) is seen as the most adaptable antenna which can be integrated with any applications [1]. One of the most attractive features of DRA is its adjustability in terms of shape, dimensions and permittivity of dielectric resonator [2-4]. As permittivity increases, the size of DRA decreases since both parameters are inversely proportional to each other. Additional advantages are various feeding methods which is strongly associated with modes being excited, wide range of dielectric constant from different dielectric materials, as well as lightweight and low loss characteristics [1,3,5,6].

Adjustability the resonant frequency is critical in DRA design. This offers a certain degree of freedom to incorporate DRA with tunable devices. A metallic plate attached to the dielectric resonator provides significant effect in varying the resonant frequency of the DRA [1,7,8]. The biggest the metallic plate on top of the DRA, the larger the shift of resonant frequency which can be obtained [9]. Besides changing the diameter

of the metal plate, varying its height can also allow changes in frequency [10]. Moreover, the height of the metal plate has greater effect towards resonant frequency of the DRA compared to the diameter. Resonant frequency of the DRA is a function of material permittivity as well as structural parameters. A set of different resonant frequencies is generated from dielectric resonators (DR) having different permittivity [11]. Adding an additive to the dielectric resonator will modify the dielectric properties of DR. In previous work [12-15], the presence of additive in $BaTiO_3$ was reported to affect the permittivity and loss tangent of DR. This in turn, influences the DRA's resonant frequency.

The common practice in producing dielectric resonators for antenna application is through the conventional solid state reaction process [16-18]. Kumazawa and Masuda [19] reported the fabrication of barium titanate thin film using sol-gel techniques. Bijumon et al. [20] reported an integrated DRA for system-on-chip applications by sol-gel composites. None were purely fabricated from sol-gel since the bulk dielectric resonator was made using wet mixing process. The sol-gel process is preferred due to its inherent advantages such as high homogeneity and purity, lower processing temperature, and fine particle size, as compared to the co precipitation and wet mixing methods [21]. However, there are very little reports about the characteristics of DRA fabricated using the sol gel method. Hence, in this paper, the compact and low profile DRA fabricated from $BaTiO_3$ material through sol gel process is reported. The effect of Nd dopant on the $BaTiO_3$ DRA performance was also investigated.

2. MATERIALS AND METHODS

A pellet was prepared from pure and Nd doped $BaTiO_3$ using the sol gel method. The value of the Nd additive was varied from 0, 0.01, 0.03, 0.05, 0.07, 0.10 and 0.13. $BaTiO_3$ powders were derived using the sol-gel method instead of the conventional method which involved mixing and milling processes. The solid state reaction of $BaTiO_3$ DR was studied by means of XRD and SEM. HP4291B RF Impedance Analyzer (1 MHz -1.8 GHz) was used to determine dielectric properties of the sample. The fabricated pellet was later attached to the grounded dielectric substrate for the completion of the DRA. The antenna structure is shown in Fig. 1. It consists of cylindrical pellets which are of radius = 10.07 mm and thickness = 1.2 mm. The pellets were placed on the 50 Ω microstrip line of length = 40 mm and width = 1.9 mm. The dimension of the microstrip line was calculated using an impedance calculation tool in the computer simulation technology (CST) software. For modeling purposes, a CST software which contains a frequency and time domain solver was used. The preferred feeding technique in this design is microstrip line due to its simplicity and direct excitation to DRA. The microstrip line had a 50 Ω impedance which was printed on a grounded substrate of permittivity ε = 3.38 and size of 50 mm × 40 mm × 0.813 mm. The positions of both DR and 50 Ω microstrip line were centered on the substrate board. To obtain optimum coupling, the position of each DR was varied provided that HEM_{11d} mode excitation was not disturbed. Once fabricated, DRA must be attached to the substrate. The air gap surface between the DRA and substrate can affect the measurement results. To do so, a nonpermanent adhesive i.e. a silicon sealant was used to bond the DRA in place. The level of this silicon sealant should be as thin as possible. The 50 Ω microstrip line is soldered to the compatible subminiature version A (SMA) connector. The measurements on resonant frequency return loss and bandwidth of DRA was done using HP8720D Network Analyzer (50 MHz to 20 GHz). Radiation patterns for both pure $BaTiO_3$ DRA and Nd doped $BaTiO_3$ DRA were also measured using Agilent Spectrum Analyzer 8565E. The first part of the measurement deals with the investigation on the pure $BaTiO_3$ pellet in DRA. The measurement consists of the modeling design, and a comparison of measurement results to highlight the potential of $BaTiO_3$ pellet synthesized via sol-gel in DRA application. Later, the same measurement used on the DRA was repeated for the Nd doped $BaTiO_3$. The amount of additive was varied and a comparison on the effect of the additive was done.

Field characteristics inside the cylindrical DRA can be analyzed using a magnetic wall model [22]. The normal mode excitation for the cylindrical DRA with direct microstrip coupling is HEM_{11d} mode. Consequently, the resonant frequency of the cylindrical DRA can be predicted from the separation equation as shown in Eq. 1 [1,22].

$$k_r^2 + k_z^2 = \varepsilon_r \left(\frac{2\pi f}{c} \right)^2 \quad (1)$$

where c is the velocity of light in free space and f is frequency. k_r and k_z are the wavenumbers inside the cylindrical DR in r and z directions, respectively. The equation is as below:

$$k_r = \frac{X_{vp}}{a} \quad (2)$$

$$k_z = \frac{(2m+1)}{2d}\pi \quad (3)$$

After rearrangement of Eq. 1, the resonant frequency of mode f_{vpm} is given as:

$$f_{vpm} = \frac{c}{2\pi\sqrt{\varepsilon_r}} \sqrt{k_r^2 + k_z^r} \quad (4)$$

and when both Eqs. 2 and 3 are substituted into Eq. 4, the theoretical resonant frequency is given as Eq. 5:

$$f_{vpm} = \frac{c}{2\pi\sqrt{\varepsilon_r}} \sqrt{X_{vp}^2 + \left[\frac{\pi a}{2d}(2m+1) \right]^2} \quad (5)$$

where X_{vp} is the root satisfying the characteristic equation.

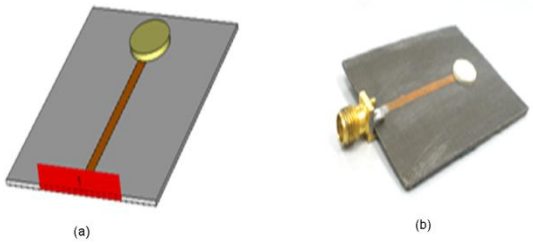

Fig. 1 Structure of the $BaTiO_3$ DRA, (a) simulated and (b) fabricated

3. RESULTS AND DISCUSSION

In order to analyze the performance of a $BaTiO_3$ pellet as the dielectric resonator in a DRA application, measurements of several parameters of the antenna were done. Fig. 2 shows simulated and measured input impedance on the Smith chart for the pure $BaTiO_3$ DRA. The range of frequency starts from 8 GHz to 10 GHz. It is noted that both impedance loops are close to the prime center of the Smith chart which represents 50 + j 0 Ω. The simulated result has an input impedance of 54.30 - j 1.70 Ω, while the measured input impedance is 48.27 - j 2.64 Ω. This shows that the DRA which utilizes the pure $BaTiO_3$ pellet has good impedance matching with the simulated one. This is because the value of measured input impedance is the closest to the prime center of the Smith chart. It shows that pure $BaTiO_3$ pellet fabricated using the sol-gel process can have good impedance matching in real antenna applications.

In correlation with the Smith chart, return loss curves are given in the Fig. 3. It shows measured and simulated return loss as a function of frequency for the DRA which uses pure $BaTiO_3$ pellet. As can be clearly

seen, the measured DRA attained a return loss of -31.18 dB at a frequency of 8.71 GHz. It gives a -15 dB bandwidth of 700 MHz or 8.03%, whereas the simulated resonant frequency shifted to the lower frequency at 8.99 GHz with -21.64 dB. The impedance bandwidth is around 380 MHz or 4.22%. As can be concluded from the curves, the significant dissimilarity between these two DRA is the impedance bandwidth.

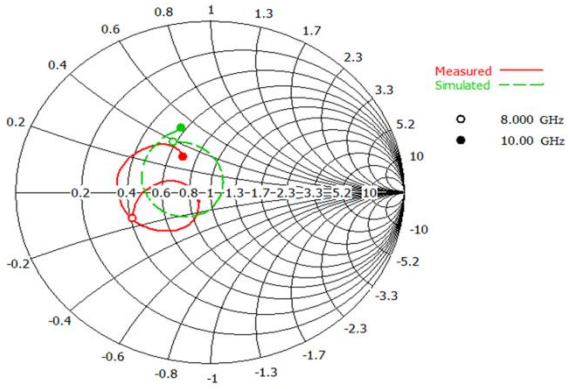

Fig. 3 Input impedance of pure $BaTiO_3$

The measured bandwidth of $BaTiO_3$ DRA is double that of the simulated bandwidth. In terms of return loss, the result shows that both measure lower than -20 dB, indicating that both DRA have low power loss. This can be related to the Smith chart as the lower the S11 curve, the closer the impedance loop to the prime center of the Smith chart. Generally, both the simulated and fabricated DRAs have different bandwidths due to tolerance of the dielectric properties and possession of different frequency resonances. Based on the S11 curves, it is proven that the $BaTiO_3$ pellet functions as a resonant structure with a specific resonant frequency. This is triggered from the internal reflections of electromagnetic waves between the air and pellet boundary. This in turn confines the energy within, and in the vicinity of the pellet, therefore forming a resonant structure [21].

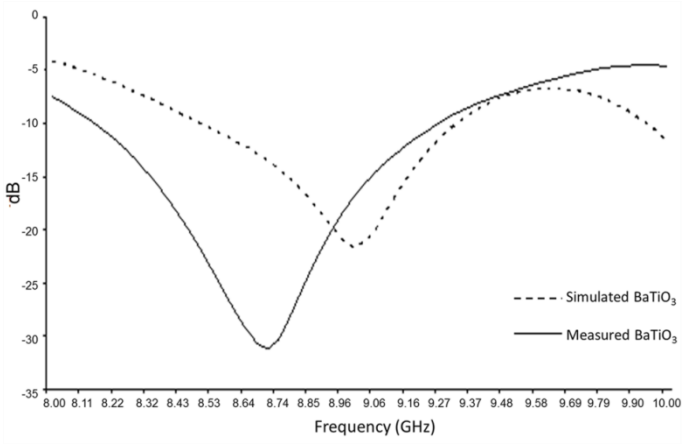

Fig. 4 Return loss of pure $BaTiO_3$ DRA

Fig. 4 shows the input impedance of pure and dopant $BaTiO_3$ DRA. All the loops are almost at the center of the Smith chart which indicates good matching for the DRA. However, it can be clearly seen that by adding dopant (Nd) into $BaTiO_3$ DR, the level of matching was improved. The loop which represents pure $BaTiO_3$ DRA is the farthest from the circle of the Smith chart, showing that it has the worst matching level with input

impedance of 48.27 - *j* 2.64 Ω at 8.71 GHz. However, for x = 0.03 and x = 0.05, the DRA has better matching. For x = 0.03, the input impedance is near to 50 Ω with 49.95 – *j* 0.02 Ω. It is almost equivalent to the 0.05 dopant $BaTiO_3$ DRA with 50.1 – *j* 0.02 Ω. Hence, it is proven that by introducing the additive Nd into $BaTiO_3$ DRA, the impedance matching of DRA can be improved.

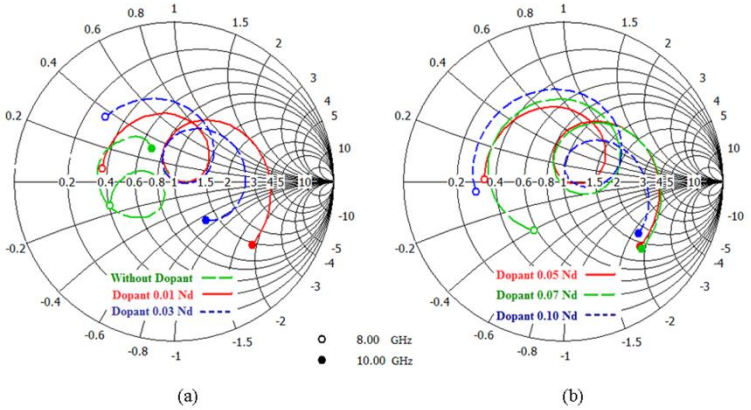

Fig. 4 Measured input impedance of doped $BaTiO_3$ DRA with (a) 0, 0.01, 0.03 Nd and (b) 0.05, 0.07, 0.10 Nd

The effect of Nd doped $BaTiO_3$ on the DRA in terms of return loss is shown in Fig. 5. It can be noted that different values of Nd as dopant resulted in different resonant frequencies. The lowest frequency belongs to the pure $BaTiO_3$ DRA at 8.71 GHz while the highest operational frequency is triggered at 9.27 GHz for 0.07 Nd $BaTiO_3$ DRA. This can be explained by the effect of permittivity values for each sample. The higher the permittivity, the lower the resonant frequency. According to our previous work [12], pure $BaTiO_3$ pellet has the highest permittivity compared to Nd doped $BaTiO_3$ pellets where the lowest permittivity was measured in the (x = 0.07) pellet. With regards to return loss, all the curves have values lower than -30 dB. It shows that all DRA achieved good matching levels at the respective frequencies where pure $BaTiO_3$ and Nd doped $BaTiO_3$ DRA performed successfully as antenna elements. The return loss for pure $BaTiO_3$ DRA is the highest with -31.18 dB, whereas all dopant $BaTiO_3$ DRA measured lower than that. In terms of bandwidth, pure $BaTiO_3$ DRA possesses the largest impedance bandwidth with 8.03%, while the x = 0.07 pellet exhibited the lowest impedance bandwidth of 3%. As expected, the presence of Nd dopant increases tan loss of $BaTiO_3$ DRA while at the same time lowers the dielectric constant. Generally, the presence of the additive Nd in $BaTiO_3$ pellet has improved the reflection coefficient of DRA, altering the resonant frequency and reduced the bandwidth of DRA.

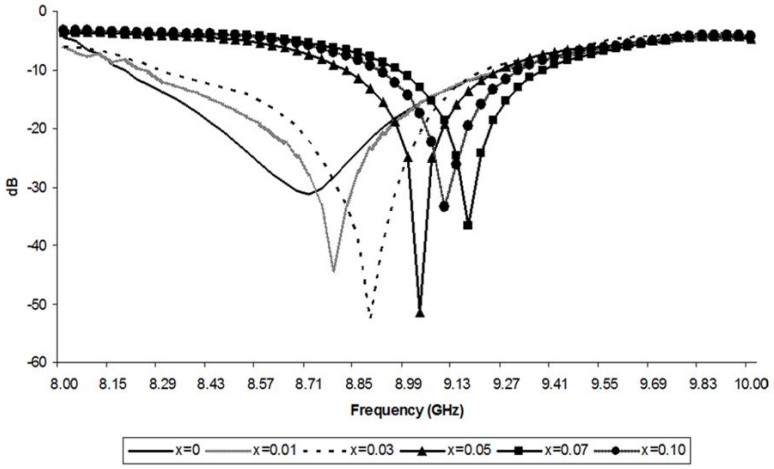

Fig. 5 Measured return loss of $BaTiO_3$ DRA with different Nd doped

4. SUMMARY

DRA using $BaTiO_3$ ceramic was designed, fabricated by means of sol-gel process and analyzed. Both simulated and measured results were presented, and it was proved that Nd-doped $BaTiO_3$ synthesized using the sol-gel process is suitable for DRA applications. The results of resonant frequency show that $BaTiO_3$ pellet is a resonant structure with $HEM_{11\partial}$ mode excitation. Good impedance matching and quasi omni directional type radiation pattern was exhibited. The presence of the additive Nd in the $BaTiO_3$ DRA changed the resonant frequency. Therefore, the $BaTiO_3$ DRA fabricated via the sol-gel process was successfully proven to be applicable in DRA.

REFERENCES

[1] A. Petosa, Dielectric resonator antenna handbook, Bolton: Artech House, (2007).

[2] Y.M.M. Antar, New directions in antenna research using dielectrics, Radio Science Conference, (NRSC 2003), Proceedings of the Twentieth National, IEEE, (2003).

[3] Y.M.M. Antar, Antennas for wireless communication: recent advances using dielectric resonators, IET Circ. Device Syst., 2 (2008) 133-138.

[4] A.A. Kishk, Dielectric resonator antenna, a candidate for radar applications, Radar Conference, Proceedings of the 2003 IEEE. IEEE, (2003).

[5] M. Cuhaci, A. Ittipoboon, A. Petosa, D. Roscoe, N. Simons, Dielectric resonator antennas as an alternative technology for PCS applications, Electrical and Computer Engineering, Canadian Conference on. Vol. 2. IEEE, (1996).

[6] S.A. Long, E.M. O'connor, The history of the development of the dielectric resonator antenna, Electromagnetics in Advanced Applications, International Conference on. IEEE, (2007).

[7] Z. Li, C. Wu, J. Litva, Adjustable frequency dielectric resonator antenna, Electron. Lett., 32 (1996) 606-607.

[8] M.T.K. Tam, R.D. Murch, Half volume dielectric resonator antenna designs, Electron. Lett., 33 (1996) 1914-1916.

[9] M.A. Saed, R. Yadla, Microstrip-fed low profile and compact dielectric resonator antennas, PIERS 2006 Cambridge: Progress in Electromagnetics Research Symposium, Proceedings, 56 (2006) 151-162.

[10] M.T. Lee, K.M. Luk, K.W. Leung, M.K. Leung, A small dielectric resonator antenna, IEEE T. Antenn. Propag., 50 (2002) 1485-1487.

[11] Z. Peng, H. Wang, X. Yao, Dielectric resonator antennas using high permittivity ceramics, Ceram. Int., 30 (2004) 1211-1214.

[12] N. Rejab, S. Sreekantan, K. Abd Razak, Z. Ahmad, Structural characteristics and dielectric properties of neodymium doped barium titanate, J. Mater. Sci. Mater. El., 22 (2009) 167-173.

[13] N. Hirose, J.M.S. Skakle, A.R. West, Doping mechanism and permittivity correlations in Nd-doped $BaTiO_3$, J. Electroceram., 3 (1999) 233-238.

[14] M.K. Rath, G.K. Pradhan, B. Pandey, H.C. Verma, B.K. Roul, S. Anand, Synthesis, characterization and dielectric properties of europium-doped barium titanate nanopowders, Mater. Lett., 62 (2008) 2136-2139.

[15] Z. Yao, H. Liu, Y. Liu, Z. Wu, Z. Shen, Y. Liu, M. Cao, Structure and dielectric behavior of Nd-doped $BaTiO_3$ perovskites, Mater. Chem. Phys., 109 (2008) 475-481.

[16] A.F.L. Almeida, R.R. Silva, H.H.B. Rocha, P.B.A. Fechine, F.S.A. Cavalcantib, M.A. Valentea, F.N.A. Freire, R.S.T.M. Sohn, A.S.B. Sombra, Experimental and numerical investigation of a ceramic dielectric resonator (DRA): $CaCu_3Ti_4O_{12}$ (CCTO, Physica B, 403 (2007) 586-594.

[17] Y.C. Chen, S.M. Tsao, C.S. Lin, Dielectric resonator antenna using $0.95MgTiO_3$ - $0.05CaTiO_3$ high permittivity ceramics, Antenna Technology: Small Antennas and Novel Metamaterials,. International Workshop on. IEEE, (2008).

[18] W. R. Stone, Classified ads available in magazine, IEEE Antenn. Propag. M., 36 (1994) 37.

[19] H. Kumazawa and K. Masuda, Fabrication of barium titanate thin films with a high dielectric constant by a sol-gel technique, Thin Solid Films**,** 353 (1999) 144-148.

[20] P.V. Bijumon, A.P. Freundorfer, M. Sayer, Y.M.M. Antar, Ultralow temperature processing and integration of dielectric resonators on silicon substrates for system-on-chip applications, IEEE T. Electron. Dev., 55 (2008), 1727.

[21] Z. Qifa, K. Anxiang, W. Longshi, Z. Taoshen, Study of solid state reactions in the PZT ceramic prepared by sol-gel technique, Properties and Applications of Dielectric Materials, 1991, Proceedings of the 3rd International Conference on. IEEE, 1991.

[22] S. Long, M. McAllister, L. Shen, The resonant cylindrical dielectric cavity antenna, IEEE T. Antenn. Propag., 31 (1983) 406-412.